Volume 14, Number 5, 2021. pp. 425-435

Jordan Journal of Physics

ARTICLE

Effect of ZrO_2 Nanofiller on the Physical Properties of Epoxy Composites: Mechanical, Thermal and Dielectric

N. Annlin Bezy[a], **A. Lesly Fathima**[b], **S. Sebastiammal**[b] and **S. Virgin Jeba**[b]

[a] *Research Scholar (Reg.No:20213042132006), Department of Physics, Holy Cross College (Autonomous), Nagercoil-629004, Tamil Nadu, India.*

[b] *Research Department of Physics, Holy Cross College (Autonomous), Nagercoil-629004, Tamil Nadu, India.*

(Affiliated to Manonmaniam Sundaranar University, Abishekapatti, Tirunelveli-627012, Tamil Nadu, India).

Doi: **https://doi.org/10.47011/14.5.4**

Received on: 01/05/2020; *Accepted on: 24/05/2021*

Abstract: In this present work, Zirconia nanoparticles were prepared by precipitation method, Zirconium Oxychloride ($ZrOCl_2.8H_2O$) and ammonia (NH_3) as starting materials. The synthesized Zirconia nanoparticles were characterized by XRD and the grain size in nanoscale was confirmed. The sheets of neat epoxy resin and epoxy with addition of ZrO_2 nanoparticles are primed by solution casting method. The structures of epoxy polymer and hardener were found out using FTIR analysis. The thermal properties were analyzed using Thermo Gravimetric Analysis (TGA) and Differential Thermal Analysis (DTA). Thermo gravimetric analysis has been employed to investigate the thermal characteristics and their mode of thermal degradation. Differential thermal analysis has been used to determine the glass transition temperature of epoxy nanocomposites. The mechanical properties like tensile and flexural studies were analyzed and thus influences of nanofiller loading on these parameters were found to be very low.

Keywords: Epoxy, ZrO_2 nanoparticles, Nanocomposites, Thermal stability, Dielectric properties, Tensile strength, Flexural strength.

Introduction

Polymer nanocomposites have attracted increasing attention in the last decade because of their significant improvement of physical and chemical properties over the matrix polymers. The effects of nanofillers on these properties have been extensively observed to make nanocomposites for application purpose. The addition of just a few percent by weight of nanofillers can result in significant enhancement in dielectric, thermal and mechanical properties. The incorporation of metal oxide nanoparticles with polymer is approached to improve the mechanical strength [1–6]. The effects of inorganic fillers on the properties of composites strongly depend on filler size and shape, type of particles and the degree of dispersion [7-8]. Various nanoscale fillers, including metal oxides, montmorillonite and calcium carbonate, have been reported to enhance the mechanical properties, thermal stability, gas barrier properties, electrical properties and flame retardancy of the polymer matrix [9-11]. Among various metal oxide fillers, nano-sized zinc oxide (ZnO), zirconium oxide (ZrO_2), titanium dioxide (TiO_2) and cerium oxide (CeO_2) fillers have attracted considerable attention because of their unique physical properties as well as their low cost and extensive applications in diverse areas [12-15]. Here, the purpose of study is to evaluate the physical properties of epoxy resin with Zirconia nanoparticles.

Corresponding Author: A. Lesly Fathima **Email**: leslysat@gmail.com

Experimental Part

X-Ray Diffraction

X-ray diffraction (XRD) was a spectroscopic method which has been used in the structure determination of crystalline materials. X-ray diffraction (XRD) of ZrO_2 nanoparticles was carried out on a XPERT – PRO diffractometer system with monochromated CuK_α (1.5406 Å) radiation working at 40 kV/30 mA. The grain size of ZrO_2 was calculated by De-bye Scherrer formula:

$$D = K\lambda/\beta cos\theta$$

where:

K is a constant;

λ is the wave length used;

β is the full width half maximum;

θ is the angle of diffraction.

Fourier Transformation Infrared Spectroscopy

Fourier Transform Infrared (FTIR) spectroscopy is used to identify organic, polymeric and in some cases inorganic materials. The FTIR analysis method uses infrared light to scan test samples and observe chemical properties. FTIR measurements for the samples were performed in SHIMADZU type IR Affinity-spectrophotometer in the range of 4000 – 400 cm^{-1}. The mode used in the FTIR characterization is transmission.

Thermal Analysis

The thermal properties were analyzed using differential scanning calorimetry and thermogravimetric analysis. Thermal stability of the nanocomposites was studied using thermogravimetric analysis (TGA) in SIINT 6300 thermogravimetric analyzer temperature ranges from 25°C to 1000°C with the heating rate of 10°C/min. Powder sample is used for thermal analysis.

Electrical Analysis

Dielectric spectroscopy was based on the phenomena of electrical polarization and electrical conduction in materials. The most common mechanisms of polarization will occur at high frequencies (10^3 Hz - 10^{15} Hz), while at very low frequencies (10^{-3} Hz – 10^3 Hz), DC conduction will become significant. Thus, dielectric spectroscopy was also well suited for the determination of both AC and DC conductivity of materials. In order to understand the influence of ZrO_2 on the dielectric property of the composites, the permittivity and dissipation factor of the composites were investigated. In the present work, the dielectric spectroscopy (DS) using the instrument HIOKI 3532-50 LCR Hitester, over a frequency range of 10^1 – 10^6 Hz, at three temperatures 50°C, 100°C and 150°C were found. For testing, the sample was cut into the dimensions of 7.5 X 6 X 4 mm. The applied voltage was set to 1V and during all the measurements, room temperature was maintained.

Mechanical Analysis

Tensile test and flexural strength test of developed sheets are performed using mechanical analyzer in tensile mode in accordance with the ASTM D-638 test standard and flexural mode with ASTM D-790 test standard, respectively. Before testing, the rectangular samples of fixed size are cut out from sheets using a clean razor blade and the upper side of cut sample for tensile test is polished to make flat surface. And the edges of the sample are polished by sand paper of a mesh of 1200. ASTM D-638 is a testing specification that determines the in-plane tensile properties of polymer matrix composite materials reinforced by high-modulus fibres. A tensile test measures the resistance of a material to a static or slowly applied force. ASTM D 790 is a method of measuring the flexural properties of plastic by setting a test bar across two supports and pushing it down in the middle until it breaks or bends at a specified distance. Flexural modulus is a measure of stiffness or rigidity.

Materials and Method

Materials

Zirconium oxychloride ($ZrOCl_2.8H_2O$) and ammonia (NH_3) purchased from Sigma Aldrich were used as starting materials for the synthesis of ZrO_2 nanoparticles. ARALDITE epoxy resin (LY 556) and hardener (HY 951) were taken as the materials for the development of polymer sheets.

Synthesis of ZrO_2 Nanoparticles

ZrO_2 nanoparticles were prepared by the precipitation method. Zirconium hydroxide precipitation ($Zr(OH)_4$) was obtained by adding

NH_3 solution drop-wise into the aqueous solution of 0.2M $ZrOCl_2.8H_2O$ at room temperature until the desired pH of 10 was reached. Zirconium hydroxide mixture was then dried in an oven at 100°C for 12 hours. Zirconia nanoparticles were obtained through calcination at 600°C for 2 hours.

Preparation of Epoxy/ ZrO_2 Nanocomposites

Epoxy resin and hardener were used in this study to develop pure and ZrO_2 nanofiller imposed epoxy nanocomposites for different ZrO_2 weight percentages (1, 3, 5 and 7) wt %. The method used in preparation of epoxy/ZrO_2 nanocomposite sample is solution casting. For pure sample, epoxy resin of 60g and hardener of 6g were poured separately in two beakers. To remove the air bubbles, both needed to be ultrasonicated for 30 minutes. After the completion of this process, the hardener was added to the epoxy resin and mixed by hand stirring. Then, it was ultrasonicated to remove air bubbles generated during the mixing process. After degassing, the mixture was poured into a metal mould. The metal mould was kept undisturbed for 1 hour at room temperature. Finally, the sample was cured by keeping the mould in an oven at 100°C for 2 hours. Thus, neat epoxy sheet was obtained. For epoxy/ZrO_2 nanocomposites, 1wt% ZrO_2 nanofillers were added with the epoxy resin and the same procedure was repeated for 3wt %, 5wt % and 7wt % ZrO_2 added epoxy nanocomposites [16-18]. The photograph of developed polymer sheets is shown in Fig.1.

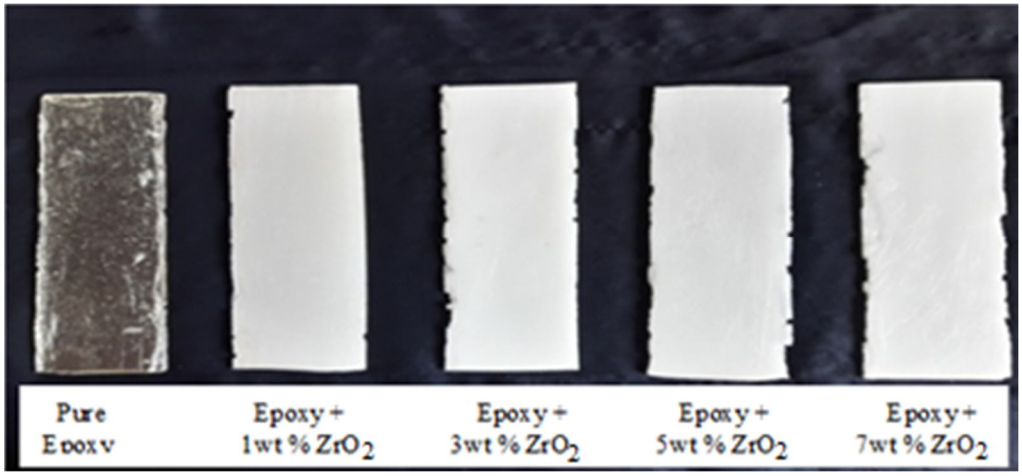

FIG. 1. Photograph of pure and ZrO_2-imposed nanocomposite sheets.

Results and Discussion

Powder X- ray Diffraction Analysis

PXRD pattern of synthesized Zirconia nanoparticles is reported in Fig.2. The XRD pattern of ZrO_2 nanoparticles is found to exhibit many diffraction peaks and of that, $(\bar{1}11)$ reflection plane is very predominant and has high intensity. The crystallite size of synthesized ZrO_2 is found to be 36.21nm and this confirms that the prepared ZrO_2 particles are in nanoscale. The X-ray diffraction spectrum confirms that the pure ZrO_2 nanopowder is in monoclinic crystalline phase. The data obtained is in good agreement with standard JCPDS file no 89-9066.

Fourier Transform Infrared Analysis

Fourier Transform Infrared spectroscopy was used to characterize the prepared pure epoxy and ZrO_2-imposed epoxy nanocomposite samples. The FTIR spectrum is shown in Fig.3 and assignments for prepared samples are listed in Table 1.

The structures of LY 556 epoxy resin and HY 951 hardener were confirmed by FTIR spectral analysis. In the FTIR spectrum of pure epoxy, the band at 3431 cm^{-1} corresponds to the vibration of hydroxyl (OH) group. The band at 3037 cm^{-1} corresponds to the CH stretching vibration in aromatic ring. The peaks at 2973 cm^{-1} and 2933 cm^{-1}indicate the asymmetric C-H stretching of CH_3 and CH_2 groups, respectively. The strong peaks at 1572 cm^{-1}, 1510 cm^{-1} and 1425 cm^{-1} indicate the C-C stretching vibration in aromatic ring. The asymmetric deformation of CH_2 produces absorption band at 1297 cm^{-1}. The asymmetric stretching of C-O in aromatic and aliphatic groups produces absorption bands at 1247 cm^{-1} and 1182 cm^{-1}, respectively. The asymmetric stretching mode of C-O-C vibration

appears at 1040 cm^{-1}. Absorption peak at 922 cm^{-1} corresponds to epoxide ring vibrations. The strong absorption peak at 828 cm^{-1} indicates C-H out-of-plane deformation in aromatic rings. The appearance of the bands at 649 cm^{-1} and 559 cm^{-1} indicates the bending vibrations of N-H and C-H, respectively. The sharpness and intensity vary for different weight percentages of ZrO_2 nanofiller-added epoxy nanocomposites. A slight shift in absorption bands is observed for ZrO_2 nanofiller-added epoxy systems. This is due to strong attraction of ZrO_2 nanoparticles with epoxy [19].

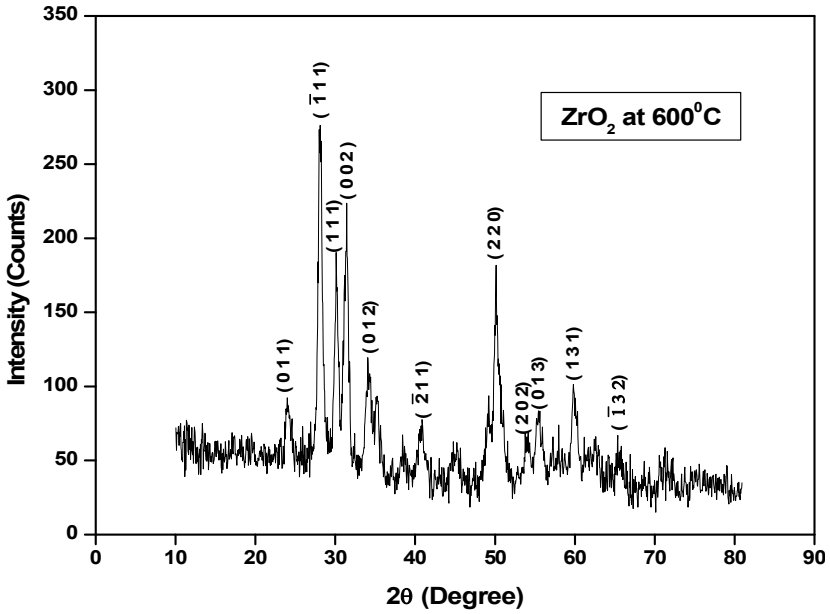

FIG. 2. XRD pattern of ZrO_2 nanoparticles.

TABLE. 1. Frequency assignments of pure and ZrO_2-epoxy nanocomposites.

Wave Number (cm^{-1})					Assignments
Pure Epoxy	Epoxy + 1wt % ZrO_2	Epoxy + 3wt % ZrO_2	Epoxy + 5wt % ZrO_2	Epoxy + 7wt % ZrO_2	
3431	3416	3433	3430	3419	O-H Stretching
3037	3036	3035	3032	3037	C-H Stretching in aromatics
2973	2971	2975	2975	2971	Asymmetric C-H Stretching of CH_3 group
2933	2932	2937	2935	2935	Asymmetric C-H Stretching of CH_2 group
1572	1572	1571	1571	1572	C-C Stretching vibration in aromatics
1510	1510	1510	1511	1510	
1425	1426	1424	1425	1426	
1297	1297	1297	1297	1297	Asymmetric CH_2 deformation
1247	1247	1247	1247	1247	Asymmetric aromatic C-O stretching
1182	1182	1182	1182	1182	Asymmetric aliphatic C-O stretching
1040	1039	1041	1042	1039	Stretching vibration of C-O-C
922	921	922	922	921	Epoxide ring vibrations
828	828	827	828	828	C-H out-of-plane deformation in aromatics
649	649	649	649	649	Bending vibration of NH
559	559	560	560	559	Bending vibration of C-H

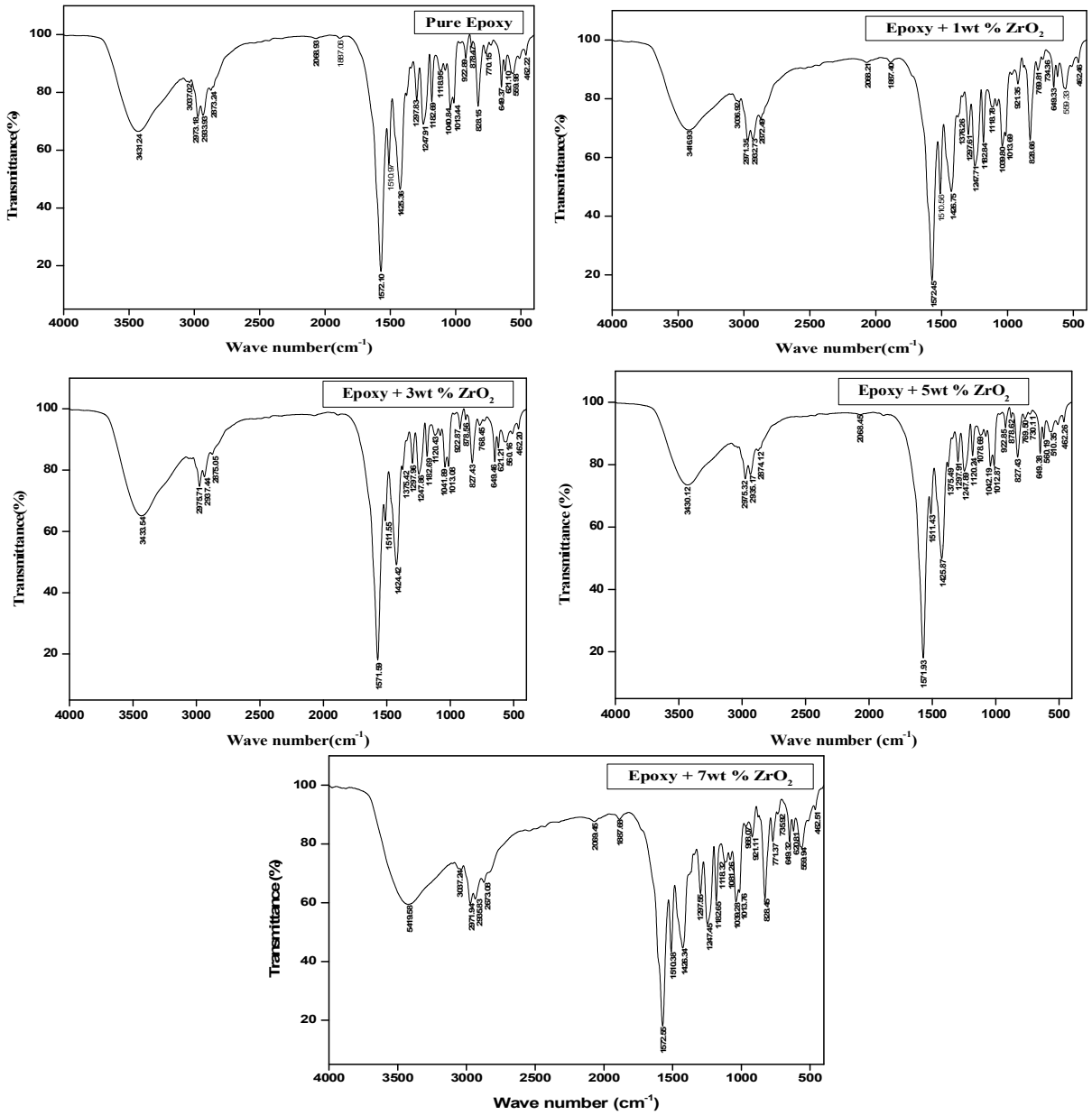

FIG. 3. FTIR spectra of pure epoxy and ZrO_2-epoxy nanocomposites.

Thermal Analysis

Thermo Gravimetric Analysis (TGA)

The thermal properties were analyzed using differential scanning calorimetry and thermogravimetric analysis. The thermo gravimetric curves are shown in Fig.4.

Both neat epoxy and ZrO_2/epoxy systems have similar decomposition profiles and the degradation takes place in two stages. Initial weight loss (weight started at 100°C) was observed in the thermograms corresponding to evaporation of water molecules from polymer samples [20]. The second step weight loss occurs due to the decomposition of polymer itself. As evident from thermograms, the nano-filler has a significant effect on thermal stability of polymers. Table 2 shows the TGA data of pure epoxy and ZrO_2-epoxy nanocomposites.

The relative thermal stability of epoxy nanocomposites has been evaluated by comparing the decomposition temperatures at different percentage weight losses. The thermal stability of the ZrO_2 nanofiller-added nanocomposites is observed to be slightly decreased as compared to that of neat epoxy. This may result from the spatial obstruction of nanoparticles on the formation of high cross-linked molecular structure of epoxy or increased free volume fractions in the polymer nanocomposites [21].

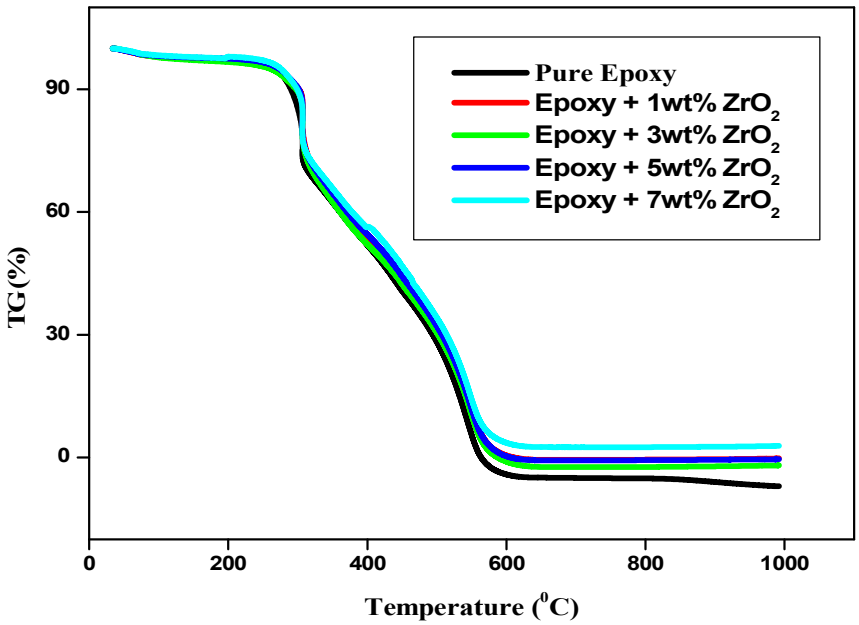

FIG. 4. Thermogravimetric curve of pure and ZrO_2-added epoxy nanocomposites.

TABLE. 2. TGA data of pure and ZrO_2-doped epoxy nanocomposites.

Sample	T_1 (T_{d1}°C)	T_2 (T_{d2}°C)
Pure Epoxy	281	507
E + 1wt%	275	500
E + 3wt%	273	489
E + 5wt%	271	509
E + 7wt%	268	504

Differential Thermal Analysis (DTA)

The DTA curves of pure and ZrO_2 imposed epoxy nanocomposites are presented in Fig. 5. It shows the effect of ZrO_2 nanoparticles on the glass transition temperature of the nanocomposites. The glass transition temperatures of pure epoxy and ZrO_2-imposed epoxy nanocomposites were listed in Table 3.

TABLE 3. Glass transition temperature of pure and ZrO_2-embedded epoxy nanocomposites.

Sample	Glass Transition temperature (T_g°C)
Neat Epoxy	71.5
E+1wt%	69.7
E+3wt%	70.7
E+5wt%	69.3
E+7wt%	70.2

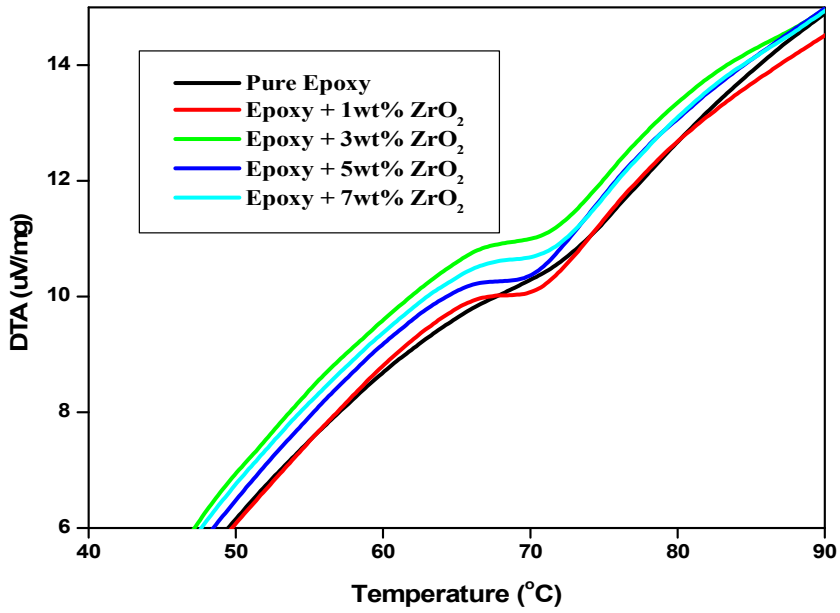

FIG. 5. DTA curves of pure and ZrO_2-added nanocomposites.

It can be ascertained from Fig. 5 that for the filler loadings, the glass transition temperature is lower than that of unfilled epoxy. The changes in T_g are due to the effect of nanoparticles only. Few studies on polymer nanocomposites have suggested that polymer nanoparticle interactions actually lead to the formation of more than one nanolayer around the nanoparticles [22].

In addition to the formation of the immobile polymer close to the particle, another polymer layer with a thickness slightly more than that of the immobile layer forms over it. The polymer segments in this extended layer are reported to be loosely bound and they relax faster causing a reduction in the nanocomposites' glass transition temperature [23].

Electrical Analysis

The variations of dielectric constant with temperature and frequency for the epoxy nanocomposites having ZrO_2 nanofillers at different filler concentrations are shown in Figs. 6-7.

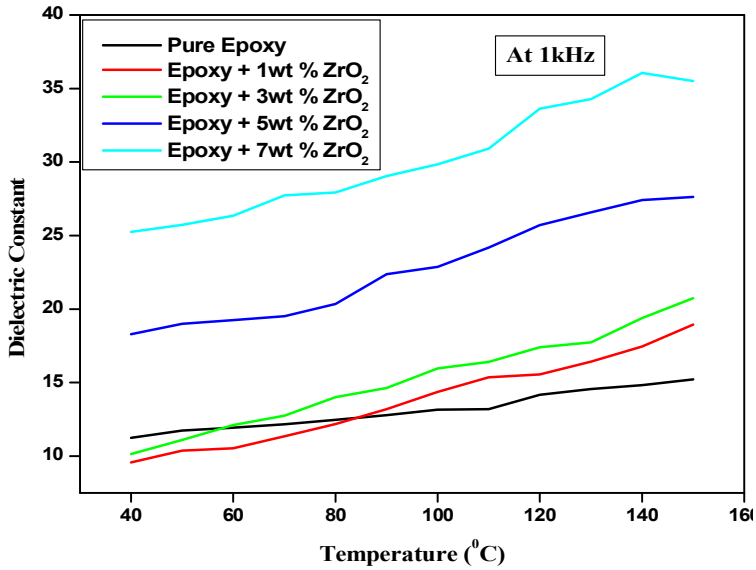

FIG. 6. Dielectric constant *vs*. temperature at 1 kHz.

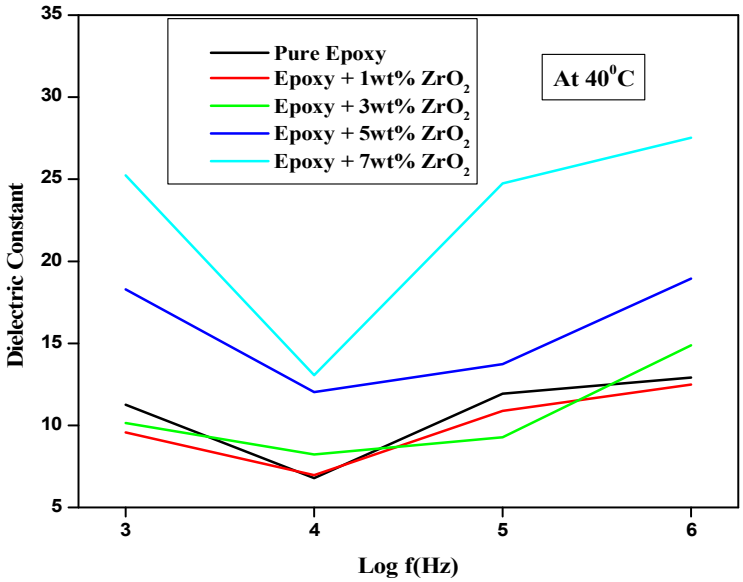

FIG. 7. Dielectric constant *vs*. frequency at 40^0C.

From Fig. 6, it can be seen that the dielectric constant increases with the increase in temperature for all the tested nanocomposites. This dependence is observed for pure and all the four filler concentrations. At low temperatures, the orientational mode cannot contribute to polarization. This leads to a lower dielectric constant at low temperatures. From Fig.7, the dielectric constant of neat and ZrO_2-imposed epoxy nanocomposites increases with increasing

frequency above 10^4 Hz. At lower frequencies of applied voltage, all the free dipolar functional groups in the epoxy chain can orient themselves resulting in a higher ε_r value at these frequencies. Further increasing frequency, the ε_r value increases. ZrO_2 displays strong ionic polarization due to Zr^{4+} and O^{2-} ions and therefore has a high value of dielectric constant [24]. In this study, it is found that 7wt% ZrO_2 nanofiller-added epoxy system has high dielectric constant.

Temperature at 1kHz, Frequency at 40^{0}C

From Fig. 8, it can be seen that the dielectric loss increases with the increase in temperature for all the tested samples. The dielectric loss values for ZrO_2 nanofiller-added epoxy nanocomposites are less than those of unfilled epoxy. From Fig. 9, pure and ZrO_2 nanofiller-added epoxy nanocomposites show that the values of dielectric loss with 1wt%, 3wt%, 5wt% and 7wt% filler concentrations are less than those of unfilled epoxy. Dielectric loss depends on the electrical conductivity in the epoxy composites. The electrical conductivity in turn depends on the number of charge carriers in the material, the relaxation time of the charge carriers and the frequency of the applied electric field. This observation is probably due to the presence of a significant number of nanoparticles in the system which influences the electrical conductivity mechanism in the nanocomposites [24].

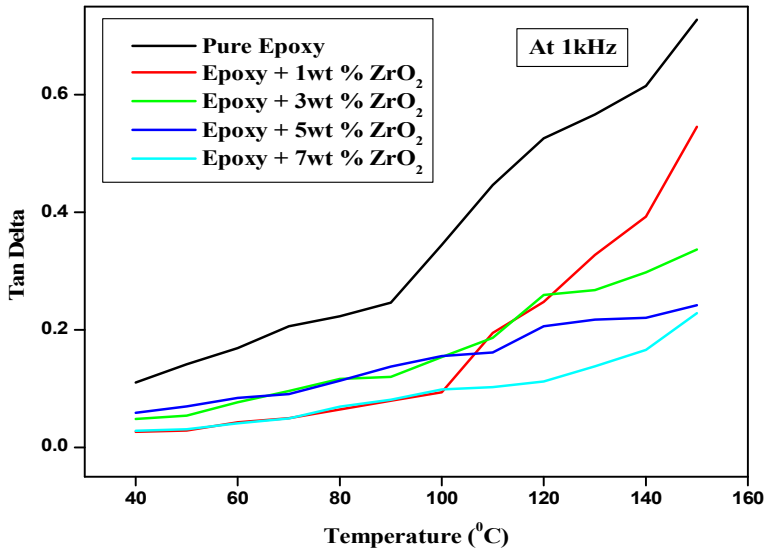

FIG. 8. Variation of tan delta *vs*. temperature at 1 kHz.

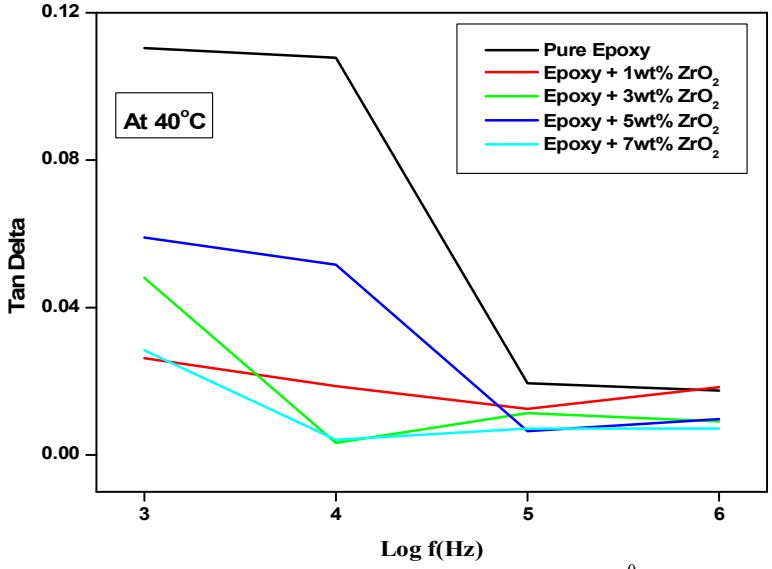

FIG. 9. Variation of tan delta *vs*. frequency at 40^{0}C.

From Fig.10, it can be seen that the AC conductivity increases with the increase in temperature for all the tested nanocomposites. Pure epoxy and ZrO_2-imposed epoxy nanocomposites show different dielectric behaviors, depending on the frequency and on the filler concentration. In our present study, the dielectric behavior is very little influenced by the type of filler and filler concentration.

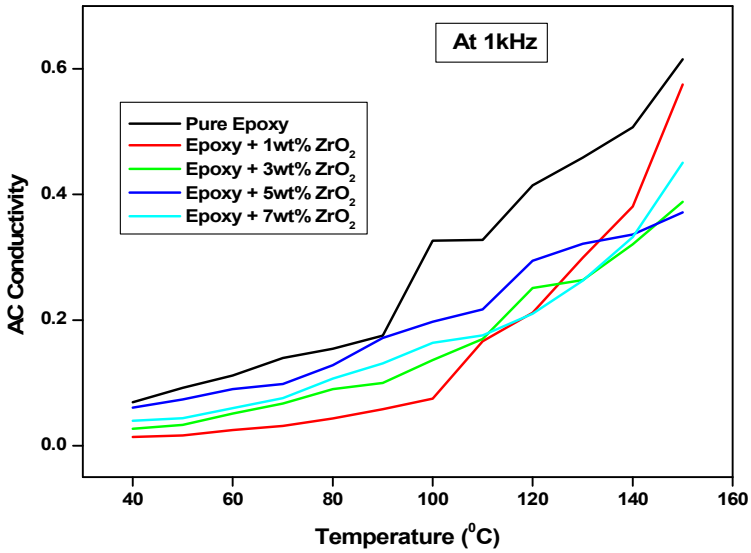

FIG. 10. Variation of AC conductivity *vs*. temperature at 1 kHz.

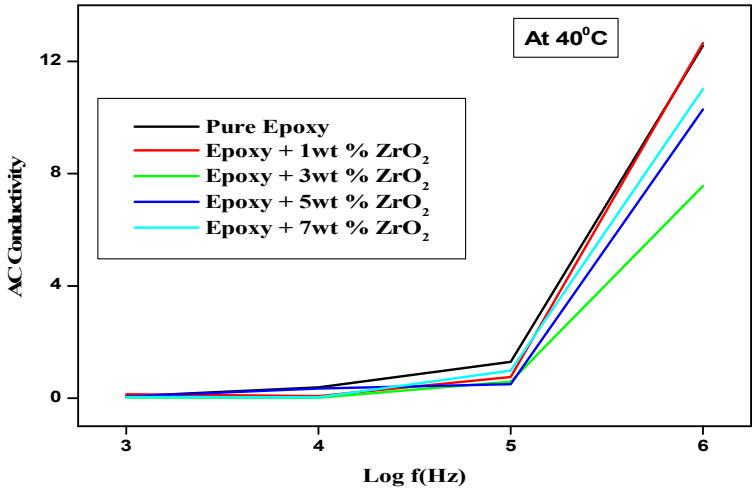

Fig. 11. Variation of AC Conductivity *vs*. Frequency at 40^0C.

Mechanical Analysis

Values of tensile strength and flexural strength for pure and ZrO_2 nanofiller (3 wt% and 5wt%) - imposed epoxy nanocomposites are shown in Table 4. It shows that the neat epoxy has maximum tensile strength. For ZrO_2 nanofiller (3wt% and 5wt%) - added epoxy nanocomposites, the tensile strength and flexural strength decreased when compared with neat epoxy. Thus, the results indicate that there may be agglomeration of nanoparticles owing to less interaction with resin [25]. Table 4 shows the values of tensile strength and flexural strength of pure epoxy and nanocomposites.

TABLE 4. Tensile strength and flexural strength.

Sample	Tensile strength (MPa)	Flexural strength (MPa)
Pure Epoxy	25.5	79.6
Epoxy + 3wt% ZrO_2	24.5	43.5
Epoxy + 5wt% ZrO_2	21.0	30.8

Conclusion

ZrO_2 nanoparticles were prepared by precipitation method. The prepared ZrO_2 nanoparticles were subjected to XRD characterization. The grain size of ZrO_2 was calculated by De-bye Scherrer formula. The grain size of synthesized ZrO_2 is found to be 36.21nm and this confirms that the prepared ZrO_2 particles are in nanoscale. Neat and ZrO_2 nanoparticles-imposed epoxy composites were synthesized by solution casting method. FTIR study proved the occurrence of epoxy and amine hardener and its interaction with ZrO_2 nanoparticles. The sharpness and intensity of the peak vary for different weight percentages of ZrO_2 nanofiller-added epoxy nanocomposites. Thermo gravimetric analysis has been employed to investigate the thermal characteristics and their mode of thermal degradation. The TGA thermograms of epoxy/ZrO_2 nanocomposites' systems exhibit lower decomposition temperature behaviours compared to neat epoxy. The glass transition temperature was determined using DTA curve and it was observed that the glass transition temperature of epoxy/ZrO_2 polymer nanocomposites decreases when compared with neat epoxy. The thermal stability was not enhanced in epoxy/ZrO_2 polymer nanocomposites when compared with neat epoxy.Dielectric properties, such as dielectric loss and dielectric constant, are evaluated to determine the electrical conductivity of prepared polymer samples. Dielectric results showed that it is a frequency-dependent parameter. For ZrO_2 nanofiller-added composites (3wt% and 5wt%), the tensile strength decreases compared with neat epoxy. Flexural strength is higher for neat epoxy when compared with ZrO_2-imposed epoxy system. This indicates that there may be agglomeration of nanoparticles owing to less interaction with resin.

References

[1] Majid, M., Hassan, E.-D., Davoud, A. and Saman, M., Composites Part B: Engineering, 42 (7) (2011) 2038.

[2] Sun, T., Chen, F., Dong, X. and Han, C.C., Polymer, 49 (11) (2008) 2717.

[3] Zhang, Q.X., Yu, Z.Z., Xie, X.L. and Mai, Y.W., Polymer, 45 (17) (2004) 5985.

[4] Luyt, A.S., Dramicanin, M.D., Antic, Z. and Djokovic, V., Polymer Testing, 28 (3) (2009) 348.

[5] Saminathan, K., Selvakumar, P. and Bhatnagar, N., Polymer Testing, 27 (3) (2008) 296.

[6] Zhao, H. and Li, R.K.Y., Polymer, 47 (9) (2006) 3207.

[7] Zaman, H.U., Hun, P.D., Khan, R.A. and Yoon, K.-B., Journal of Reinforced Plastics and Composites, 31 (5) (2012) 323.

[8] Chan, C.-M., Wu, J., Li, J.-X. and Cheung, Y.-K., Polymer, 43 (10) (2002) 2981.

[9] Galgali, G., Agarwal, S. and Lele, A., Polymer, 45 (17) (2004) 6059.

[10] Alexandre, M. and Dubois, P., Mater. Sci. Eng.: R: Reports, 28 (1-2) (2000) 1.

[11] Motha, K., Hippi, U., Hakkala, K, Peltonen, M., Ojanperä, V., Löfgren, B. and Seppälä, J., J. Appl. Polym. Sci., 94 (3) (2004) 1094.

[12] Chatterjee, A., J. Appl. Polym. Sci., 116 (6) (2010) 3396.

[13] Li, Y.J., Duan, R., Shi, P.B. and Qin, G.G., J. Crystal Growth, 260 (3-4) (2004) 309.

[14] Zeng, D.W., Xie, C.S., Zhu, B.L., Song, W.L. and Wang, A.H., Mater. Sci. Eng.: B, 104 (1-2) (2003) 68.

[15] Yang, Y., Chen, H., Zhao, B. and Bao, X., J. Crystal Growth, 263 (1-4) (2004) 447.

[16] Sumi, E., Virgin Jeba, S. and Lesly Fathima, A., Archives of Physics Research, 6 (1) (2015) 20.

[17] Annlin Bezy, N. and Lesly Fathima, A., International Journal of Engineering Research and General Science, 3 (5) (2016) 143.

[18] Lesly Fathima, A., International Journal of Engineering and General Science, 5 (2) (2017) 10.

[19] Mahulikar, P.P., Jadhav, R.S. and Hundiwale, D.G., Iranian Polymer Journal, 20 (5) (2011) 367.

[20] Liu, Y.L., Hsu, C.Y., Wei, W.L. and Jeng, R.J., Polymer, 44 (18) (2003) 5159.

[21] Zhu, J., Wei, S., Ryu, J., Sun, L., Luo, Z. and Guo, Z., ACC Appl. Mater. Interfaces, 2 (7) (2010) 2100.

[22] Gupta, A.K., Balakrishnan, V.R. and Tiwary, S.K., International Journal of Polymer Technology, 1 (2-3) (2009) 181.

[23] Tsagaropoulos, G. and Eisenberg, A., Macromolucules, 28 (18) (1995) 6067.

[24] Singha, S. and Thomas, M.J., IEEE Transaction on Dielectrics and Electrical Insulation, 15 (1) (2008) 12.

[25] Merad, L., Benyousef, B., Abadie, M. and Charless, J.P., Journal of Engineering and Applied Sciences, 6 (3) (2011) 205.